© 2017. Published by The Company of Biologists Ltd | Journal of Experimental Biology (2017) 220, 1729-1736 doi:10.1242/jeb.154781

RESEARCH ARTICLE

Modulation of upper limb joint work and power during sculling while ballasted with varying loads

Jessy Lauer[1,2,*], Annie Hélène Rouard[2] and João Paulo Vilas-Boas[1]

ABSTRACT

The human musculoskeletal system must modulate work and power output in response to substantial alterations in mechanical demands associated with different tasks. In particular, in water, upper limb muscles must perform net positive work to replace the energy lost against the dissipative fluid load. Where in the upper limb are work and power developed? Is mechanical output modulated similarly at all joints, or are certain muscle groups favored? This study examined, for the first time, how work and power per stroke are distributed at the upper limb joints in seven male participants sculling while ballasted with 4, 6, 8, 10 and 12 kg. Upper limb kinematics was captured and used to animate body virtual geometry. Net wrist, elbow and shoulder joint work and power were subsequently computed through a novel approach integrating unsteady numerical fluid flow simulations and inverse dynamics modeling. Across a threefold increase in load, total work and power significantly increased from 0.38±0.09 to 0.67±0.13 J kg^{-1}, and 0.47±0.06 to 1.14±0.16 W kg^{-1}, respectively. Shoulder and elbow equally supplied >97% of the upper limb total work and power, coherent with the proximo-distal gradient of work performance in the limbs of terrestrial animals. Individual joint relative contributions remained constant, as observed on land during tasks necessitating no net work. The apportionment of higher work and power simultaneously at all joints in water suggests a general motor strategy of power modulation consistent across physical environments, limbs and tasks, regardless of whether or not they demand positive net work.

KEY WORDS: Swimming, Kinetics, Load, Inverse dynamics, Computational fluid dynamics

INTRODUCTION

Humans move in water, sometimes undulating ventrally and ricocheting at the surface when swimming butterfly, sometimes paddling dorsally in a windmill-like fashion when swimming backstroke, in addition to the more unusual yet utilitarian forms of locomotion used by lifeguards or combat swimmers, lying on one side and recovering the arms under the water. Regardless of the style adopted, the arms are swept through the water to generate thrust. This requires that substantial net mechanical work be performed by upper limb muscles to replace the energy lost against the dissipative load of the water. As the load increases (for example, by increasing steady swimming speed, or artificially by using ballast, as in di Prampero et al., 1974), task mechanical requirements must be met by proportional increases in mechanical work and power per stroke. How does the musculoskeletal system adapt to accommodate the changing mechanical demands of the environment? Where does the increased power come from? Is the mechanical work output modulated similarly at the shoulder, elbow and wrist or are certain muscle groups favored? This study sought to provide the answers to such questions by comparing net joint work and power during sculling performed under varying mechanical loads. Sculling is the action of sweeping the arms back and forth, typically describing the shape of a ∞. This is an integral part of swimming strokes, incorporating flow phenomena responsible for high force production (Takagi et al., 2014), and an exercise frequently used in fitness and rehabilitation programs. Sculling is thus an upper limb movement well suited to the broad study of work and power modulation in water.

Mechanical power output has been previously calculated through ingenious methods (semi-tethered swimming: Dominguez-Castells et al., 2013; MAD system: Toussaint et al., 1990; dry-land ergometry: Swaine, 2000), yet none capture the instantaneous power directly apportioned by the upper limb musculature or explain work and power production within the limb itself. We recently developed a novel approach integrating inverse dynamics and unsteady fluid flow simulations to examine upper limb aquatic movement kinetics for the first time from a joint-level perspective (Lauer et al., 2016). This approach nicely complements the more macroscopic, above-mentioned approaches, as it provides further insight into how muscle groups are recruited to meet the demands of the environment.

Certain muscle groups may function differently from others, and contribute unevenly to overall mechanical requirements. Such a 'division of labor' in terms of work performance mainly reflects the distribution of muscle mass within a limb (Biewener, 2016). High work output is generally observed in large muscles distributed proximally, whereas low work output is seen distally in smaller muscles. Studies of avian muscle function during flight support this regional specialization in the functional role of muscle groups. Just as humans move their arms for hydrodynamic propulsion, birds generate aerodynamic lift to power flight by moving their wings through large excursions. Rapid wing flap is achieved by large proximal muscles shortening over a significant fraction of their resting fiber length, producing considerable work (Biewener, 2011). Small muscles located at the elbow operate over shorter strains to control wing shape and orientation, yet show both work production and absorption (Robertson and Biewener, 2012). In the human upper extremity, muscle mass is also concentrated proximally (Holzbaur et al., 2007) and can be expected to provide the majority of work. However, experimental studies are needed as no data for upper limb joint work when moving in water are available.

[1]Center of Research, Education, Innovation and Intervention in Sport, Faculty of Sport; and Porto Biomechanics Laboratory, University of Porto, 4200-450 Porto, Portugal. [2]Inter-university Laboratory of Human Movement Science, University Savoie Mont Blanc, 73376 Le Bourget-du-Lac, France.

*Author for correspondence (jessy.lauer@gmail.com)

J.L., 0000-0002-3656-2449

Received 13 December 2016; Accepted 17 February 2017

Journal of Experimental Biology (2017) 220, 1729-1736 doi:10.1242/jeb.154781

List of symbols

$\bar{P}^{+}$	average mechanical power produced at a joint
$\bar{P}^{-}$	average mechanical power absorbed at a joint
$\bar{P}^{+}_{tot}$	total power produced by the upper limb
$\bar{P}^{-}_{tot}$	total power absorbed by the upper limb
W^{+}	positive work done at a joint during a stroke
W^{-}	negative work done at a joint during a stroke
W^{+}_{tot}	total positive work done by the upper limb
W^{-}_{tot}	total negative work done by the upper limb

The human musculoskeletal system must consistently alter its performance to accommodate changing mechanical demands associated with different steady tasks. These steady tasks require steady work input, as opposed to non-steady tasks, which require transient changes in muscle work for just one or a few strides, such as during stabilization (Daley et al., 2007). Although the way in which this challenge is accomplished in water remains obscure, on land, it is relatively well understood. During level walking and running up to ∼7 m s^{-1}, demands for increased positive work per stride are achieved by increasing in parallel the work done by all lower limb muscle groups (Farris and Sawicki, 2012b; Schache et al., 2015). By contrast, sprinting, accelerating and incline running necessitate a different control strategy, as they involve a redistribution of work and power output proximally to the hip (Qiao and Jindrich, 2016; Roberts and Belliveau, 2005; Schache et al., 2015). However, unlike level steady-speed locomotion, these tasks have the peculiarity that they are associated with a net positive work requirement and/or a change in limb posture that requires the hip muscles to do greater work (Roberts and Belliveau, 2005); hence the suggestion that task net work requirement might be an important indicator of how humans meet overall mechanical demands (Farris and Sawicki, 2012b).

This study aimed to test, for the first time, two fundamental hypotheses relative to upper limb aquatic movement mechanics. Based upon the relative distribution of muscle mass within the human upper limb, it was first predicted that the majority of the work and power would be produced proximally at the shoulder and elbow. Second, as aquatic movements naturally require that net positive work be done against the dissipative load of the water, it was expected that higher mechanical demands would be met by redistributing upper limb work output proximally to the shoulder muscles.

MATERIALS AND METHODS

Participants and experimental procedure

Experiments were carried out on seven male participants (27.7±5.8 years, 1.82±0.05 m, 77.8±6.5 kg). Ethical approval was granted by the University of Porto review board, and all participants provided written informed consent prior to testing. They performed sculling motion in the middle of a 25 m-long, 2 m-deep indoor swimming pool so as to remain vertically still with the head above the water for about 10 s. Use of the legs was not allowed. To manipulate the demand for mechanical work per stroke, participants were randomly ballasted with 4, 6, 8, 10 and 12 kg tied around the waist (see Fig. 1 for illustration of the task). While ballasted with 14 kg, only two participants managed to keep their head above the water. However, they did so for less than 5 s. These trials were discarded, as they were not deemed representative of a task requiring steady work input; 12 kg was therefore regarded as the maximum load participants could sustain. Rest periods of 3 min were observed between each condition.

Fluid flow simulations and inverse dynamics analysis

The quantification of joint kinetics during underwater movements rests on a new approach integrating computational fluid dynamics (CFD) and inverse dynamics modeling. The methodology involved four steps. First, 3D upper limb joint kinematics was recorded by automatically tracking the trajectories of 12 markers positioned along the upper limb and thorax (xiphoid process, suprasternal notch, C7, T8, acromion, lateral and medial epicondyles, ulnar and radial styloids, third and fifth metacarpals, and an additional piece of reflective tape at the tip of the middle finger) with a 12-camera underwater motion capture set-up sampling at 100 Hz (Oqus 3 and 4 series, Qualisys, Gothenburg, Sweden). Markers at C7, acromion and medial epicondyle were temporarily invisible because of proximity with the water surface or occlusion by the chest when bringing the arms forwards. Missing information represented up to ∼75 frames (at most 6.7% of the trial duration), distributed in short individual gaps of ∼10 frames (∼100 ms). These were filled with Qualisys Track Manager software built-in spline interpolation. Kinematic data were digitally filtered using a zero-lag fourth-order Butterworth filter with a cut-off frequency of 6 Hz. Four strokes, selected on the basis of minimal xiphoid process vertical displacement, were retained for processing. Segment coordinate systems (thorax, upper arm, forearm and hand) were subsequently constructed in agreement with the International Society of Biomechanics convention (Wu et al., 2005). Second, body virtual geometries were obtained from a Mephisto 3D scanner (4DDynamics, Antwerp, Belgium), edited and converted into a CAD model prior to import into ANSYS® Fluent® release 14.5 CFD software (ANSYS, Inc., Canonsburg, PA, USA). Third, the numerical simulation was set and the virtual model was animated. Difficulties arise when numerically controlling joint deformation as the geometry is highly constrained. Joints must connect smoothly to the adjacent rigid surfaces throughout the motion to avoid negative cell volumes and to prevent the simulation from stopping before completion. We implemented a dual quaternion smooth skinning

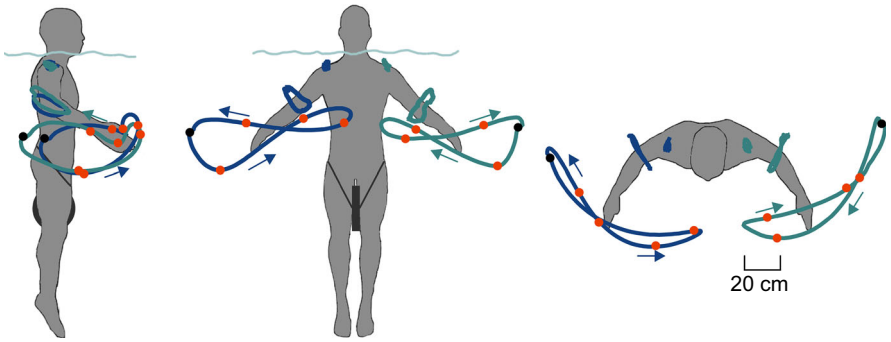

Fig. 1. Kinematic traces of the tip of the middle finger, elbow joint center and acromion during sculling. These were averaged over four cycles from one participant sculling to maintain his head above the water surface while ballasted with 4 kg (blue) and 12 kg (green). Recordings are from the right arm only, but are represented on both sides for illustration purposes from lateral, front and top perspectives. Black dots indicate where the movement starts, with red dots spaced every 20% of stroke duration.

Journal of Experimental Biology

Journal of Experimental Biology (2017) 220, 1729-1736 doi:10.1242/jeb.154781

algorithm in C programming language to handle complex 3D deformations, a task that is otherwise unfeasible in Fluent®. Each of the vertices forming the ~40,000 upper limb facets was individually displaced based on kinematic data input and an additional weighted transformation ensuring skin-like animation of flexible body parts. This in turn allowed the quantification of hydrodynamic forces acting upon the entire upper limb in dynamic conditions. The instantaneous resultant hydrodynamic force on a segment was evaluated by integrating the pressure and shear stress acting on each individual facet over the segment surface. Knowing the position vector of all facet centroids at each time point, the average location of the pressure (i.e. the instantaneous center of pressure) was readily computed. Segment buoyancy and its point of application were determined from virtual model volume, whereas segment mass, center of mass and moments of inertia were estimated from scaling equations based on subject anthropometry (Dumas et al., 2007). Fourth, these data were fed into an inverse dynamics model of the upper limb to compute net joint moments. The model was implemented through the homogeneous matrix approach (Legnani et al., 1996), a mathematical notation derived from robotics that is convenient for computer applications, suitable for the modeling of complex joints and has low sensitivity to kinematic measurement error (Doriot and Chèze, 2004).

Joint power and work computation

Joint angular velocity was obtained by subtracting the angular velocity of the proximal segment from that of the distal one. Instantaneous 3D joint power was readily calculated as the dot product of the net joint moment and joint angular velocity vectors, and normalized to body mass. Shoulder, elbow and wrist power time series were integrated with respect to time over discrete periods of positive and negative power, yielding the positive work W^+ and negative work W^- done per stroke at each upper limb joint. W^+_{tot} and W^-_{tot} were calculated as the sum of W^+ and W^- done at each joint, respectively. W^+ and W^- were further divided by stroke duration to give the average positive $\bar{P}^+$ and negative $\bar{P}^-$ joint power. $\bar{P}^+_{tot}$ and $\bar{P}^-_{tot}$ were calculated in the same manner as W^+_{tot} and W^-_{tot}. In order to determine whether a change in mechanical demand influenced individual joint relative contributions to $\bar{P}^+_{tot}$ and $\bar{P}^-_{tot}$, $\bar{P}^+$ and $\bar{P}^-$ at each joint were respectively expressed as a percentage of $\bar{P}^+_{tot}$ and $\bar{P}^-_{tot}$. Furthermore, joint angular excursions (i.e. the difference between the minimum and maximum angles of a given joint over a stroke) and peak joint moments were measured to indirectly evaluate the mechanisms by which joint mechanical work was altered (Arnold et al., 2013; Roberts and Scales, 2004).

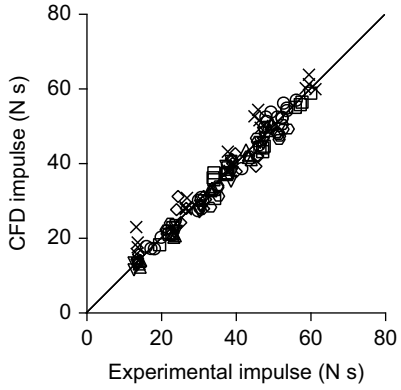

Fig. 2. Impulse generated by the arms plotted against the net ballast impulse. Simulation accuracy was tested by regressing the impulse calculated from integrating over a cycle of external force vertical components computed through computational fluid dynamics (CFD) onto the net ballast impulse. Numerical output fell on the identity line (slope of the major axis regression β=1.00, 95% confidence interval 0.97–1.03), giving confidence in the results. Symbols identify different participants.

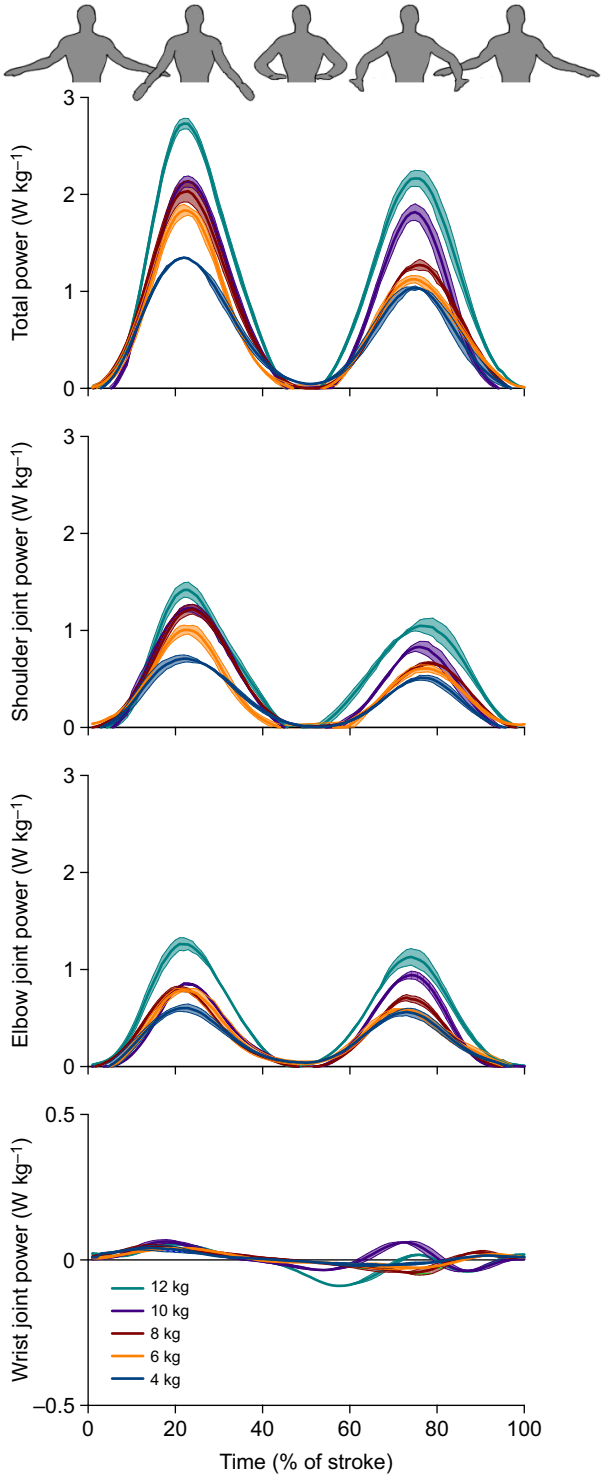

Fig. 3. Representative instantaneous total, shoulder, elbow and wrist joint power normalized to a single stroke for each of the five loading conditions. Results are means±s.d. (shaded bands) obtained from four strokes in each condition from participant 3. Note the different *y*-axis scale for the wrist plot. At the top, silhouettes show one sculling cycle, with maximum power generation when the arms are moved side-to-side and null power at stroke reversal.

Journal of Experimental Biology (2017) 220, 1729-1736 doi:10.1242/jeb.154781

Statistical analysis

Statistical tests were run in R 3.3.2 (https://www.R-project.org/), with a significance level of 0.05. Four cycles per participant and condition were analyzed. Data were time-normalized as a percentage (0–100%) of a single stroke. Simulation accuracy was tested with a major axis regression, comparing the impulse delivered by the arms (calculated through CFD from integrating external force vertical components) with the net body+ballast impulse. It was calculated as the product of stroke period and the sum of ballast weight and net body buoyancy (taken as the extra load necessary to immerse the body just below the surface after maximal inspiration). The simulations were considered accurate if the 95% confidence interval of the slope β of the major axis included 1 (Rayner, 1985). Distribution normality was checked with the Shapiro–Wilk test. Mixed-effects models (via the R package lme4; Bates et al., 2015) were used to detect any main effect of the magnitude of the mechanical demand on the work and power generated, individual joint relative contributions, joint angular excursions and peak moments. Load condition was treated as a fixed effect and individual as a random effect. Provided that a significant effect was found, *post hoc* Tukey pairwise contrasts with Bonferroni adjustment for multiple comparisons were conducted to identify which conditions were significantly different from each other.

RESULTS

The slope of the major axis regression between the numerically and experimentally calculated vertical impulse was β=1.00 (Fig. 2), with a 95% confidence interval of 0.97–1.03. As the mechanical demand increased, so did the magnitude of the instantaneous power at all joints (Fig. 3), with a measured peak power output of 2.7±0.4 W kg^{-1} at the highest load. This was reflected in W^{+} and $\bar{P}^{+}$ done at the upper limb joints (Fig. 4). Specifically, a significantly higher amount of W^{+} and $\bar{P}^{+}$ was being generated at the shoulder and elbow, whereas no change was observed at the wrist. As a result, W^{+}_{tot} and $\bar{P}^{+}_{tot}$ increased markedly from 0.38±0.09 to 0.67±0.13 J kg^{-1} ($F_{4,6}$=57.46, P<0.001), and 0.47±0.06 to 1.14±0.16 W kg^{-1} ($F_{4,6}$=140.24, P<0.001), respectively. Levels of W^{-}_{tot} and $\bar{P}^{-}_{tot}$ were negligible (on average <0.02±0.01 J kg^{-1} and 0.04±0.02 W kg^{-1}), representing less than 3.5% of the total upper limb work and power. The wrist contributed 1.8–2.4% to W^{+}_{tot} and $\bar{P}^{+}_{tot}$ (Fig. 5). In contrast, the shoulder and elbow were the main contributors, equally supplying on average 22 times more work and power (respectively, 47.5–52.5% and 45.6–50.0%). Mixed-effects models revealed no significant effect of mechanical loading on individual joint relative contributions (Fig. 5). Representative joint angular kinematics and joint moments are shown in Fig. 6. During sculling, shoulder and elbow angular excursions were much greater than those at the wrist, notably about the axes of flexion/extension and adduction/abduction, though with no visible changes with load (Fig. 6A). Conversely, increasingly high joint moments were produced with increasing load, peaking at ∼25% and 75% of the stroke (Fig. 6B). Angular excursion remained unchanged about all joint degrees of freedom, whereas peak moments showed significant increases in magnitude at all joints as the mechanical demand rose (Fig. 7).

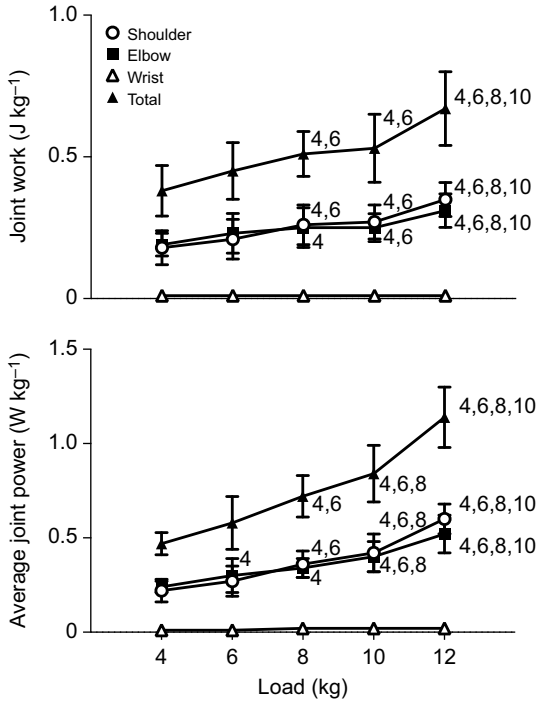

Fig. 4. Mechanical work (top) and average power (bottom) at the shoulder, elbow and wrist as the mechanical load increases. Elbow and shoulder joints exhibited parallel, significant increases in work and power by ∼75% and 150%, respectively. Error bars represent 1 s.d. Significant difference (P<0.05) from the 4, 6, 8 and 10 kg load conditions is indicated by the corresponding numbers.

DISCUSSION

Upper limb joint work and power distribution

We sought to analyze through a novel integrative approach how joint work and power are modulated during upper limb aquatic movements in response to substantial changes in mechanical demand. Simulations were accurate, judging by the slope of the major axis, thus giving confidence in the results. We tested two hypotheses. First, we hypothesized that the majority of the work and power would be produced at the shoulder and elbow given the proximal concentration of large muscles. This hypothesis was confirmed. We found that muscle groups crossing the shoulder and elbow supplied >97% of work and power. This is consistent with the proximo-distal gradient of work performance apparent in the limbs of many terrestrial vertebrate animals, for which evolutionary pressures have favored work modulation by proximal muscles (Biewener and Daley, 2007). Here, we report that such a gradient also exists within the human upper limb when moving in a complex, fluid physical environment. Moreover, muscle groups at the shoulder and elbow contributed mechanical demands equally, and

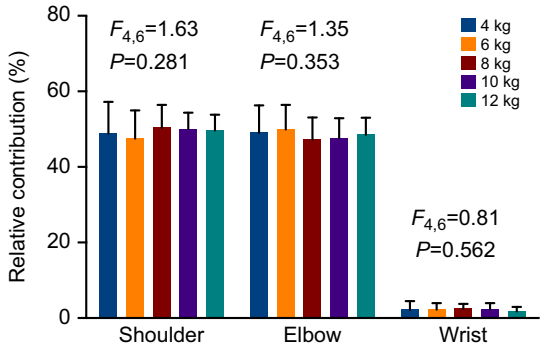

Fig. 5. Individual joint relative contributions to the total average power and work produced by the upper limb. Across a threefold increase in load, no power redistribution occurred within the upper limb. Error bars represent 1 s.d.

Journal of Experimental Biology (2017) 220, 1729-1736 doi:10.1242/jeb.154781

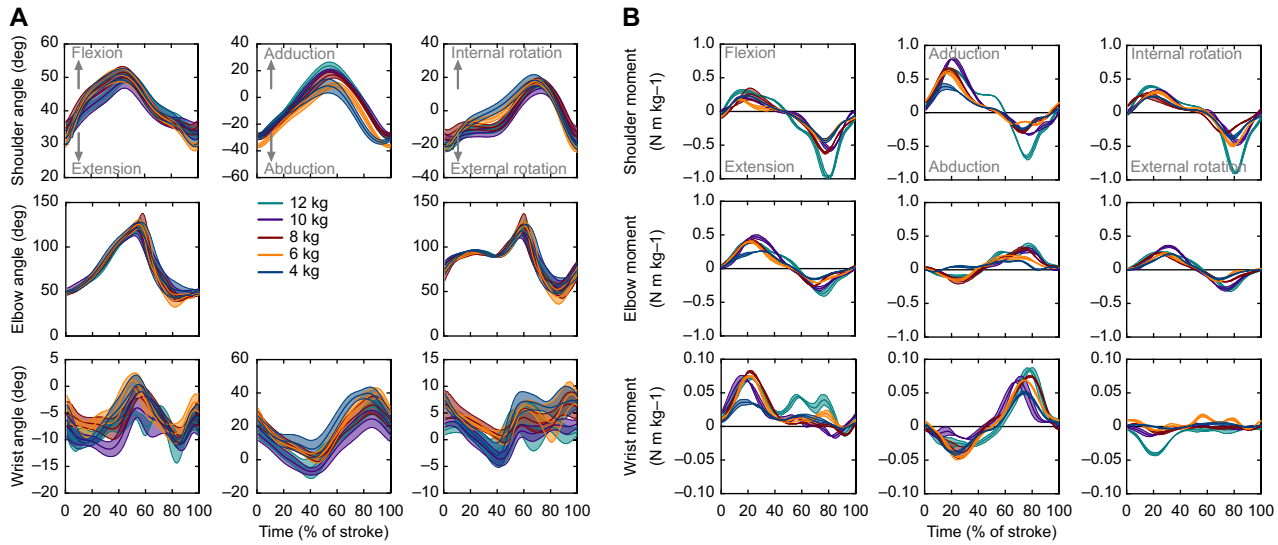

Fig. 6. Average 3D upper limb joint kinematics and joint moments plotted over a stroke. Shoulder (top), elbow (middle) and wrist (bottom) joint kinematics (A) and kinetics (B) were projected onto non-orthogonal coordinate systems so that individual components reflected mechanical actions about the axes of flexion/extension (left column), adduction/abduction (center) and internal/external rotation (right). Elbow adduction/abduction was left blank as this degree of freedom was constrained. Means±s.d. are shown for participant 3 from four strokes in each condition, illustrating typical stroke-to-stroke variability.

are therefore of equal importance in the underwater production of force.

The second hypothesis was that increasing mechanical demands would be met by redistributing upper limb work output proximally to shoulder muscles as net positive work must be done against the dissipative load of the water. This hypothesis was rejected, as individual joint relative contributions were observed to remain constant when mechanical demands were substantially altered. Across a threefold increase in load (4–12 kg), elbow and shoulder joints exhibited parallel increases in work and power by ∼75% and 150%, respectively. Curiously, this behavior is also observed during steady, level terrestrial locomotion (Farris and Sawicki, 2012b; Schache et al., 2015), the net mechanical work requirement of which is, however, negligible. Our results therefore suggest a transversal motor strategy of power modulation across physical environments, limbs and tasks, regardless of whether or not they demand net positive work. Previous findings of proximal redistribution of work and power output that occurred when accelerating (Qiao and Jindrich, 2016), sprinting (Schache et al., 2015) and incline running (Roberts and Belliveau, 2005) might thus have been confounded by postural constraints altering muscle effective mechanical advantage, rather than reflecting an actual neuromuscular response. This is further exemplified by the work of Farris and Sawicki (2012a) on the distribution of lower limb joint work during hopping across various frequencies. Even though no net work is required by the task, a proximal shift in work production from the ankle to the knee was observed as mechanical demands increased (i.e. decreasing hop frequency), due mostly to a more flexed knee posture. This adds to the fact that the power modulation neuromotor strategy might be partially hidden by constraints imposed by the task.

Invariant joint relative contributions to total work and power lend support to the idea that complex movements are controlled modularly, i.e. the central nervous system adopts a simple control scheme in which a few sets of invariant muscle synergies or ‘modules’ act as building blocks to simplify motor coordination and accomplish complex motor tasks (e.g. d’Avella et al., 2003). For example, walking mechanics under different mechanical demands can be robustly reproduced through tuning module recruitment intensity alone (McGowan et al., 2010). Although muscle activity was not recorded here, we can speculate that complex aquatic movements are similarly governed. To respond to the increased demand for mechanical work, it may be that modules simply get more activated, with the result that work output proportionately increases at all joints. Further investigations are needed to test this assumption.

The work performed by a muscle during contraction is the product of the force developed and the distance shortened. Increased mechanical work output can thus be achieved through either producing higher forces or shortening more, which would be apparent in increases in joint moments or joint excursions (Arnold et al., 2013; Roberts and Scales, 2004). Increasing the mechanical work output of the upper limb musculature to accommodate increasing mechanical demands in water was primarily done through twofold increases in moments at all joints, rather than sweeping the arms over greater joint excursions: angular excursions remained unchanged with load. Assuming that muscle shortening and muscle force output are respectively proportional to joint angular excursion and peak joint moment, our results suggest that increased work was likely done by muscles producing higher forces.

Constraints to human upper limb performance in water

An insignificant amount of power was being absorbed over a stroke (<3.5% of the total generated power) regardless of the load, indicating a negligible dissipation or storage of energy in anatomical structures. This is unlike flying animals, for example, that store and release wing inertial energy in the tendon of pectoralis (amounting to 18% of the positive work the muscle performs) to aid the upstroke to downstroke transition (Biewener, 2011). The existence of springs in swimming vertebrates is much more controversial. While skin deformation and axial skeleton bending were found to provide such mechanical advantages (Pabst, 1996), there is only a little, indirect evidence in whales and dolphins that tendons might serve energy-saving roles (Alexander, 2002). A modeling study of paddling ducks revealed that they do not operate in a resonance-like mode,

Journal of Experimental Biology (2017) 220, 1729-1736 doi:10.1242/jeb.154781

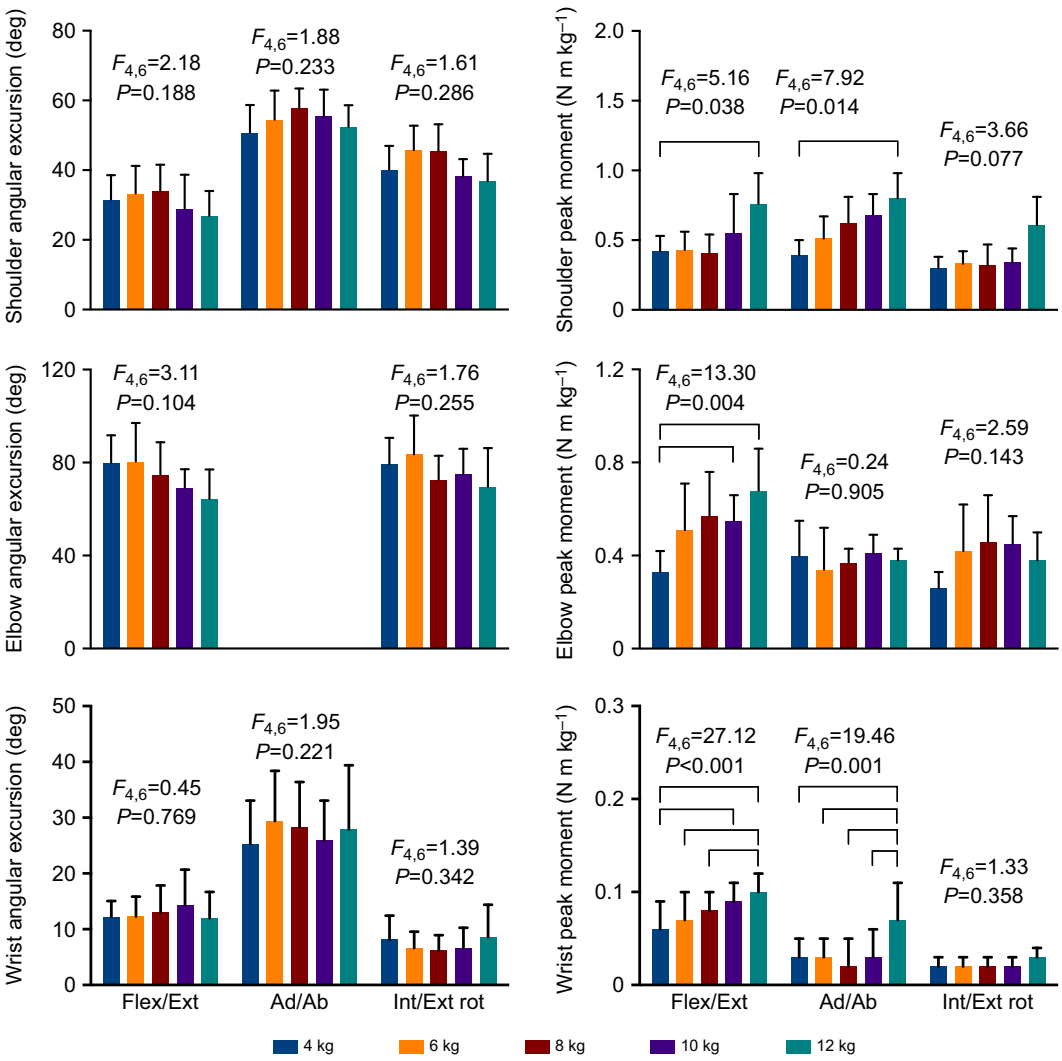

Fig. 7. Upper limb joint angular excursion (left) and peak moment (right) as a function of mechanical load. Data are presented as means±s.d. about each degree of freedom at the shoulder (top), elbow (middle) and wrist (bottom). Elbow adduction/abduction was left blank as this degree of freedom was constrained. Significant pairwise differences (P<0.05) are indicated by horizontal bars. Joint work output was increased primarily by increasing joint moment rather than joint excursion. Flex/Ext, flexion/extension; Ad/Ab, adduction/abduction; Int/Ext rot, internal/external rotation.

concluding that the musculoskeletal system of drag-based swimmers does not behave like a spring (Clark and Fish, 1994). Furthermore, for a high ratio of fluid to inertial load, power amplification was predicted not to occur in a simple muscle–tendon complex because of the phase delay of drag (Richards and Sawicki, 2012). Only modest enhancement was theoretically possible for artificial musculoskeletal design parameters, bringing additional proof that elastic energy storage only rarely benefits aquatic locomotor performance. Likewise, in humans moving in water, the nature of the medium itself – which is highly dampening and entails a substantial loss of energy to overcome drag on the appendages – likely limits the usefulness of elastic mechanisms in powering cyclical aquatic movements. Thus, performance is directly determined by the maximal work and power theoretically available from muscle mass.

We can ask whether work and power production measured here fall within the theoretical capacities of vertebrate skeletal muscles. Participants were performing at maximum effort, as increasing load beyond 12 kg could not be steadily supported. Considering an average mass of shoulder and elbow muscles of 3 kg (Holzbaur et al., 2007), we can extrapolate to a total muscle mass-specific work and average power of ∼17 J and 30 W kg^{-1} muscle, respectively. Under optimal conditions of shortening range and speed, those values are respectively 4 and 2.5–8 times less than the estimated maximum capacity for work and power production of rapidly contracting striated muscle (Biewener et al., 1998; Peplowski and Marsh, 1997; Weis-Fogh and Alexander, 1977). This suggests a constraint to overall human upper limb mechanical performance in water, most likely as a result of upper body morphology specialized for overhead throwing (Roach et al., 2013).

Limitations and future research

The present study has limitations that ought to be acknowledged. The analysis of joint work and power through inverse dynamics only provides an indirect measure of muscle–tendon function as these variables represent the net effect of all the muscles, tendons, ligaments and contact forces at that joint (Farley and Ferris, 1998). Work and power estimates can be flawed as a result of: (i) energy storage in elastic structures that allows negative work in one phase to be recovered as positive work in a subsequent phase; (ii) muscle co-contraction causing the net moment at a joint to be less than the sum of flexor and extensor moments; and (iii) intercompensation

of joint power by biarticular muscles (Sasaki et al., 2009). The first has been found to be insignificant, and thus does not constitute a relevant source of error. To confirm whether the second affects the current findings would require muscular activity recordings. However, according to previous EMG studies in swimming (Caty et al., 2007; Lauer et al., 2013), we can expect muscle co-contraction to momentarily occur at the wrist and elbow. As a result, wrist and elbow joint work calculated here might slightly underestimate the actual musculotendon work (by ∼7–14%, on the basis of calculations during walking; Sasaki et al., 2009); this would not alter our main conclusions. Neglecting the third mechanism has been shown, in fact, to yield more accurate muscle work estimates during pedaling (Neptune and van den Bogert, 1997) and walking (Sasaki et al., 2009). The extent to which this holds true in aquatic movements further warrants the use of muscle-actuated forwards dynamics simulations.

Summary

Using a novel integrative approach coupling CFD and inverse dynamics, we investigated how the human musculoskeletal system adapted to substantial changes in mechanical demands when performing in water. Shoulder and elbow muscle groups equally contributed to >97% of the total work and power. As observed on land, increasing mechanical requirements were met by the apportionment of higher work and power simultaneously at all joints, suggesting a general motor strategy of power modulation consistent across physical environments, limbs and tasks, regardless of whether or not they demand positive net work. Higher mechanical work output was achieved through increasing net joint moments rather than joint angular excursion. Total upper limb work and power were found to be well below the theoretical limit of striated muscle work and power production, likely because of an anatomical constraint to overall human upper limb mechanical performance in water. This study offers the first insight into the modulation of upper limb work and power at the joint level in water, and encourages muscle-driven forwards dynamics modeling studies to examine further the limiting factors of underwater power production.

Competing interests

The authors declare no competing or financial interests.

Author contributions

J.L., A.H.R. and J.P.V.-B. designed the study. J.L. conducted the experiment. J.L., A.H.R. and J.P.V.-B. interpreted the data. J.L. drafted the manuscript. J.L., A.H.R. and J.P.V.-B. edited the manuscript and approved the submitted version.

Funding

This research received no specific grant from any funding agency in the public, commercial or not-for-profit sectors.

References

Alexander, R. M. (2002). Tendon elasticity and muscle function. *Comp. Biochem. Physiol. A Mol. Integr. Physiol.* **133**, 1001-1011.
Arnold, A. S., Lee, D. V. and Biewener, A. A. (2013). Modulation of joint moments and work in the goat hindlimb with locomotor speed and surface grade. *J. Exp. Biol.* **216**, 2201-2212.
Bates, D., Mächler, M., Bolker, B. and Walker, S. (2015). Fitting linear mixed-effects models using lme4. *J. Stat. Soft.* **67**, 1-48.
Biewener, A. A. (2011). Muscle function in avian flight: achieving power and control. *Philos. Trans. R. Soc. Lond. B Biol. Sci.* **366**, 1496-1506.
Biewener, A. A. (2016). Locomotion as an emergent property of muscle contractile dynamics. *J. Exp. Biol.* **219**, 285-294.
Biewener, A. A. and Daley, M. A. (2007). Unsteady locomotion: integrating muscle function with whole body dynamics and neuromuscular control. *J. Exp. Biol.* **210**, 2949-2960.
Biewener, A., Corning, W. and Tobalske, B. (1998). In vivo pectoralis muscle force-length behavior during level flight in pigeons (Columba livia). *J. Exp. Biol.* **201**, 3293-3307.
Caty, V., Aujouannet, Y., Hintzy, F., Bonifazi, M., Clarys, J. P. and Rouard, A. H. (2007). Wrist stabilisation and forearm muscle coactivation during freestyle swimming. *J. Electromyogr. Kinesiol.* **17**, 285-291.
Clark, B. D. and Fish, F. E. (1994). Scaling of the locomotory apparatus and paddling rhythm in swimming mallard ducklings (Anas platyrhynchos): Test of a resonance model. *J. Exp. Zool.* **270**, 245-254.
Daley, M. A., Felix, G. and Biewener, A. A. (2007). Running stability is enhanced by a proximo-distal gradient in joint neuromechanical control. *J. Exp. Biol.* **210**, 383-394.
d'Avella, A., Saltiel, P. and Bizzi, E. (2003). Combinations of muscle synergies in the construction of a natural motor behavior. *Nat. Neurosci.* **6**, 300-308.
di Prampero, P. E., Pendergast, D. R., Wilson, D. W. and Rennie, D. W. (1974). Energetics of swimming in man. *J. Appl. Physiol.* **37**, 1-5.
Dominguez-Castells, R., Izquierdo, M. and Arellano, R. (2013). An updated protocol to assess arm swimming power in front crawl. *Int. J. Sports Med.* **34**, 324-329.
Doriot, N. and Chèze, L. (2004). A three-dimensional kinematic and dynamic study of the lower limb during the stance phase of gait using an homogeneous matrix approach. *IEEE Trans. Biomed. Eng.* **51**, 21-27.
Dumas, R., Chèze, L. Verriest, J.-P. (2007). Adjustments to McConville et al. and Young et al. body segment inertial parameters. *J. Biomech.* **40**, 543-553.
Farley, C. T. and Ferris, D. P. (1998). Biomechanics of walking and running: centre of mass movements to muscle action. *Exerc. Sport Sci. Rev.* **26**, 253-286.
Farris, D. J. and Sawicki, G. S. (2012a). Linking the mechanics and energetics of hopping with elastic ankle exoskeletons. *J. Appl. Physiol.* **113**, 1862-1872.
Farris, D. J. and Sawicki, G. S. (2012b). The mechanics and energetics of human walking and running: a joint level perspective. *J. R. Soc. Interface* **9**, 110-118.
Holzbaur, K. R. S., Murray, W. M., Gold, G. E. and Delp, S. L. (2007). Upper limb muscle volumes in adult subjects. *J. Biomech.* **40**, 742-749.
Lauer, J., Figueiredo, P., Vilas-Boas, J. P., Fernandes, R. J. and Rouard, A. H. (2013). Phase-dependence of elbow muscle coactivation in front crawl swimming. *J. Electromyogr. Kinesiol.* **23**, 820-825.
Lauer, J., Rouard, A. H. and Vilas-Boas, J. P. (2016). Upper limb joint forces and moments during underwater cyclical movements. *J. Biomech.* **49**, 3355-3361.
Legnani, G., Casolo, F., Righettini, P. and Zappa, B. (1996). A homogeneous matrix approach to 3D kinematics and dynamics — I. Theory. *Mech. Mach. Theory* **31**, 573-587.
McGowan, C. P., Neptune, R. R., Clark, D. J. and Kautz, S. A. (2010). Modular control of human walking: adaptations to altered mechanical demands. *J. Biomech.* **43**, 412-419.
Neptune, R. R. and van den Bogert, A. J. (1997). Standard mechanical energy analyses do not correlate with muscle work in cycling. *J. Biomech.* **31**, 239-245.
Pabst, D. A. (1996). Springs in swimming animals. *Am. Zool.* **36**, 723-735.
Peplowski, M. M. and Marsh, R. L. (1997). Work and power output in the hindlimb muscles of Cuban tree frogs Osteopilus septentrionalis during jumping. *J. Exp. Biol.* **200**, 2861-2870.
Qiao, M. and Jindrich, D. L. (2016). Leg joint function during walking acceleration and deceleration. *J. Biomech.* **49**, 66-72.
Rayner, J. M. V. (1985). Linear relations in biomechanics: the statistics of scaling functions. *J. Zool.* **206**, 415-439.
Richards, C. T. and Sawicki, G. S. (2012). Elastic recoil can either amplify or attenuate muscle-tendon power, depending on inertial vs. fluid dynamic loading. *J. Theor. Biol.* **313**, 68-78.
Roach, N. T., Venkadesan, M., Rainbow, M. J. and Lieberman, D. E. (2013). Elastic energy storage in the shoulder and the evolution of high-speed throwing in Homo. *Nature* **498**, 483-486.
Roberts, T. J. and Belliveau, R. A. (2005). Sources of mechanical power for uphill running in humans. *J. Exp. Biol.* **208**, 1963-1970.
Roberts, T. J. and Scales, J. A. (2004). Adjusting muscle function to demand: joint work during acceleration in wild turkeys. *J. Exp. Biol.* **207**, 4165-4174.
Robertson, A. M. B. and Biewener, A. A. (2012). Muscle function during takeoff and landing flight in the pigeon (Columba livia). *J. Exp. Biol.* **215**, 4104-4114.
Sasaki, K., Sasaki, K., Neptune, R. R. and Kautz, S. A. (2009). The relationships between muscle, external, internal and joint mechanical work during normal walking. *J. Exp. Biol.* **212**, 738-744.
Schache, A. G., Brown, N. A. T. and Pandy, M. G. (2015). Modulation of work and power by the human lower-limb joints with increasing steady-state locomotion speed. *J. Exp. Biol.* **218**, 2472-2481.
Swaine, I. L. (2000). Arm and leg power output in swimmers during simulated swimming. *Med. Sci. Sports Exerc.* **32**, 1288-1292.
Takagi, H., Shimada, S., Miwa, T., Kudo, S., Sanders, R. and Matsuuchi, K. (2014). Unsteady hydrodynamic forces acting on a hand and its flow field during sculling motion. *Hum. Mov. Sci.* **38**, 133-142.

Toussaint, H. M., Knops, W., de Groot, G. and Hollander, A. P. (1990). The mechanical efficiency of front crawl swimming. *Med. Sci. Sports Exerc.* **22**, 402-408.
Weis-Fogh, T. and Alexander, R. M. (1977). The sustained power output from striated muscle. In *Scale Effects in Animal Locomotion* (ed. T. J. Pedley), pp. 511-525. London: Academic Press.
Wu, G., van der Helm, F. C. T., (DirkJan) Veeger, H. E. J., Makhsous, M., Van Roy, P., Anglin, C., Nagels, J., Karduna, A. R., McQuade, K. J., Wang, X. et al. (2005). ISB recommendation on definitions of joint coordinate systems of various joints for the reporting of human joint motion–Part II: shoulder, elbow, wrist and hand. *J. Biomech.* **38**, 981-992.